Egypt. J. Chem. **Vol. 66**, No. 3. pp. 233 - 243 (2023)

Egyptian Journal of Chemistry

http://ejchem.journals.ekb.eg/

Practiced Synthesis and Biological Evaluation of Some New Pyrimidin-2-Thione Derivatives as Potential Anticancer Agents

Omnia S. Abdel Zaher [2], Monda M. M. Badawy [3], Mohamed R. Aly[2], Sameh A. Rizk[1*]

[1]*Chemistry Department, Faculty of Science, Ain Shams University, Abassia, Cairo 11566, Egypt*

[2]*Chemistry Department, Faculty of Science, Port-Said University, Port Said, Egypt*

[3]*Health Radiation Research Department, National Center for Radiation Research and Technology, (NCRRT), Egyptian Atomic Energy Authority (EAEA), Cairo, Egypt.*

Abstract

An efficient new method has been established for the synthesis of new nucleoside by Biginelli reaction of 2-pyrrole-carbaldehdye, ethyl 3,5-dioxohexanoate and thiourea. The titled compound was submitted to react with ethyl chloroacetate and chloroacetyl chloride under different conditions to afford some novel nucleosides as anticancer agents. Hydrazinolysis of the pyrimidin-2-thione was studied under different conditions. The synthesized compounds were evaluated for their anticancer activity and was found to exhibit promising activities. All new compounds were tested for possible anti-cancer activity against HepG-2 cell lines in comparison to the reference drug doxorubicin (DOX). Compound 10 was the most active against the liver carcinoma cell line (HepG-2) giving promising half-maximal inhibitory concentration (IC50) value of 25.5±1.3 µg/mL, compared with DOX with IC50 value of 0.36±0.02 µg/mL. However, it has weak cytotoxic effects against normal rat hepatocytes with 50% cytotoxic concentration (CC50) = 1877.5 µg/ml (= > 500 µg/ml). Compound 10 was selected to be tested in combination with ionizing gamma radiation. Gene expression levels of the cell cycle inhibitor p21 and caspase-3 was quantified. As well as, Oxidative stress was quantified by measuring the concentration of malondialdehyde (MDA), and antioxidant activity of reduced gluthatione (GSH). This study concluded that the new derivative of the Pyrimidin-2-Thione compound has an effective anti-cancer effect, and it was found that using the new compound with ionizing radiation at a dose of 8 Gy improves the effectiveness of the compound on liver cancer cells.

Key Words: Pyrimidin-2-Thione, Ionizing radiation, Anticancer activity, p21 and Caspase-3.

1. Introduction

Tetrahydropyrimidinones and pyrazoles are an important classes of compounds due to their therapeutic and pharmacological properties, e.g. anti-inflammatory, antihypertension, anticancer and antimicrobial activities [1,2]. The common synthetic routes to these compounds generally involve multi-step transformations that are essentially based on the Biginelli condensation methodology. Multicomponent reactions constitute major importance in organic synthesis because of its diversity, efficiency and quick access to highly functionalized organic molecules which make them significant in drug discovery process [i,ii,iii]. Prompted by these observations and in continuation of our search [iii,iv,v,vi], we herein report the synthesis of title compound using microwave (MW) energy. Recently a major development that had a profound impact on heterogeneous reactions is the use of MW irradiation techniques. This approach has been used for a variety of applications in organic synthesis and functional group transformations. MW assisted heating under controlled conditions is an invaluable technology because it often dramatically reduces reactions times, typically from days or hours to minutes or even seconds [vii,viii].

Cancer drug targeting is an effective way to treat malignancies or cancer growths. Chemotherapy can be used either individually or in conjunction with other interventions, such as surgery or radiation. Radiotherapy uses high frequency penetrating waves like x-rays or gamma rays, or particles like proton rays or neutron rays to kill or prevent the replication of cancer cell. Pyrimidine has been documented to possess anticancer activity, in a similar manner, pyrazolo[1,5-a] pyrimidine motifs derivatives are essential biomolecule in cancer treatment [ix].

*Corresponding author e-mail: samehrizk2006@gmail.com.

Receive Date: 21 June 2022, Revise Date: 14 July 2022, Accept Date: 18 July 2022

DOI: 10.21608/EJCHEM.2022.146115.6357

Among the various mechanisms to control the cancer cells; inducing apoptosis and suppress the proliferation of cancer cells by arresting the cell cycle in phase G0 / G1, phase G2 / M [x,xi].

Apoptosis is a crucial cytotoxicity condition caused by anticancer drugs[xii]. Apoptosis or programmed cell death is a natural process that maintains a balance between cell proliferation and cell death and plays a regulatory role in regulating cell population size and homeostasis of tissues[xiii]. Apoptosis avoidance is known to be one of the hallmarks of cancer cells [xiv] Caspases, a family of proteolytic enzymes is well known to play a crucial role in the apoptotic process. Activating these proteases which are usually present inside cells as inactive zymogens result in the cleavage of several protein substrates inside the cell leading to irreversible apoptotic cell death. Caspase-3 among these is one of the most powerful downstream caspases and is called Caspase Effector [xv]. Also, cyclin-dependent kinase inhibitors p21and p27 are proteins that bind and inhibit the activity of complexes of CDK2 / cycline E, CDK4 / cycline D1, and/or CDK6 / cycline D1 and thus regulate the progression of the cell cycle at phase G1[xvi].

Glutathione exists in both reduced (GSH) and oxidized (GSSG) states. GSH is one of the major endogenous antioxidants produced by the cells, participating directly in the neutralization of free radicals and reactive oxygen compounds, as well as protecting cellular protein thiol groups and maintaining exogenous antioxidants such as vitamins C and E in their reduced (active) forms [xvii]. Therefore, GSH is critical to fight against oxidative stress [xviii].

Malondialdehyde (MDA) is a lipid peroxide that can damage the plasma membrane of cells. By measuring its content, we can usually understand the degree of lipid peroxidation in the body, thereby indirectly evaluating the degree of cell damage [xix, xx].

1. Material and Methods:

2.1. Experimental Section

General: All melting points were measured on a Gallenkamp electric melting point apparatus and are uncorrected. The FTIR spectra (ν, cm^{-1}) were recorded using potassium bromide disks on Fourier Transform Infrared Thermo Electron Nicolet iS10 Spectrometer (Thermo Fisher Scientific Inc., Waltham, MA, USA) at the Central Laboratory of Faculty of Science, Ain Shams University. The ^{13}C and ^{1}H-NMR spectra (δ_H, ppm) were run at 100 and 400 *MHz* on BRUKER 400 BB NMR Spectrometer (BRUKER, Manufacturing & Engineering Inc., Anaheim, CA, USA) using tetramethyl silane (TMS) as internal standard in deuterated dimethylsulfoxide (DMSO-d_6) at Faculty of Pharmacy, Ain Shams University. The mass spectra (MS) were recorded on Shimadzu GC-MS-QP-1000 EX mass spectrometer (Shimadzu Scientific Instruments, Inc., USA) operating at 70 eV at the regional center for Mycology and Biotechnology of Al-Azhar University, Nasr City, Cairo, Egypt. Sonication (Toshcon model SW 4 cleaner, 37 kHz, 150 W) achieved the synthesized compounds. Check the purity of synthesized compounds with thin-layer chromatography (TLC) using Merck Kiesel gel 60 F_{254} analytical sheets obtained from Fluka. All chemicals and solvents used were obtained from commercial sources and used as received or dried by standard procedures.

General procedure for the synthesis of pyrimidin-2-thione 2

Method I:

An equimolar mixture of pyrrole-2-aldehyde , thiourea and ethyl 3,5-dioxohexanoate (5 mmol) in *N*,*N*-dimethlformamide (10 ml) containing 2-drops of concentrated sulfuric acid was heated on oil bath at 140-150^{o}C for 2 h. After cooling, the reaction mixture was poured onto ice-cold water. The separated solid was filtered off, dried and recrystallized from benzene to afford pyrimidinethione **2**.

Method II:

Sonicate a mixture of pyrrole aldehyde (1 mmol), thiourea and ethyl 3,5-dioxohexanoate together in a mortar and then transfer into 10 mL of ethanol in round-bottom flask located in an ultrasonic cleaning bath with Emax measured at 30°C. Reaction progress sustained until the reactants disappeared by TLC. Irradiation at 20–25 min afforded yellow solid product, decanted with crushed ice, dried, and recrystallized.

7-methyl-4-(1H-pyrrol-2-yl)-2-thioxo-1,2,3,4-tetrahydro-5H-pyrano[4,3-d]pyrimidin-5-one (2)

Brown crystals, mp. 210-212^{o}C, yield 81%. IR: 3377, 3223 (2 NH), 1712 (C=O), 1622 (C=N), 1185 (C=S). ^{1}H-NMR: 11.24-10.21 (bs, 1H, NHCS pyrim, exchangeable D_2O), 9.73 (s, 1H, NH pyrrole, exchangeable D_2O), 6.55-7.01 (m, 3H, pyrrole-H), 5.48 (s, 1H, C_2-H pyrone), 2.37 (s, 3H, CH_3 pyrone).^{13}C-NMR: 195.0 (C=O), 174.3 (C=S), 150.8 (C=C), 144.4 (C=N), 139.7, 133.2, 130.0, 129.0, 128.9, 128.5, 128.4, 126.9, 125.0, 124.0, 119.0, 118.9 (Ar-C), 66.8 (CH), 30.7 (CH_3). EIMS (*m/z*, %): 262 (M+3, 22), 259 ($M^{\cdot+}$, 99), 215 (25), 193 (33). Anal. Calc. for $C_{12}H_9N_3O_2S$ (259.14): C, 55.59; H, 3.50; N, 16.21; S, 12.36. Found: C, 55.34; H, 3.28; N, 16.11; S, 12.18.

Synthesis of 8-methyl-3,6-dioxo-5-(1H-pyrrol-3-yl)-2,3-dihydro-6H-pyrano[4,3-d]thiazolo[3,2-a]pyrimidin-4-ium chloride (4)

A solution of pyrimidinethione **2** (2 mmol), ethyl chloroacetate (2.1 mmol) and freshly prepared

anhydrous sodium acetate or potassium carbonate (2 mmol) in dry acetone (20 ml) was heated under reflux for 24 h, respectively. After solvent evaporator, the oil product **3** was collected and solidify via treatment with drops HCl (0.5 mL) to furnish thiazolopyrimidine **4** that recrystallized from ethanol as yellow crystals, recrystallized from ethanol to afford compound **4** (identity: melting point, mixed melting point, TLC and IR). mp. 240-242ºC, yield 63%. IR: 1712 (C=O Pyrone), 1707 ($N^+C=O$), 1602 (C=N). ^{1}H-NMR: 8.49-7.31 (m, 3H, Ar-H), 5.16 (s, 1H, C_4-H pyrimidine), 5.29, 4.77 (s, 1H, NH pyrrole), 4.50 (s, 2H, CH_2), 3.20 (s, 3H, CH_3CO), 2.15 (s, 3H, CH_3C-N). ^{13}C-NMR: 197.6 (C=O), 172.1 (C=O), 158.4 (C=N), 130.1, 129.9, 129.4, 129.2, 129.0, 123.7, 119.9, 113.8 (Ar-C), 66.5 (CH), 39.8 (CH_2), 31.1 (CH_3). EIMS (*m/z*, %): 428 ($M^{\cdot+}$, 24), 400 (32), 387 (100), 367 (63), 326 (67), 267 (36), 219 (40), 191 (28), 158 (44), 124 (58), 115 (57), 88 (42). Anal. Calcd. for $C_{14}H_{10}ClN_3O_3S$ (335.13): C, 50.08; H, 3.00; Cl, 10.56; N, 12.52; S, 9.55. Found: C, 49.89; H, 2.95; Cl, 10.37; N, 12.31, S, 9.41.

Hydrazinolysis of pyrimidinethione 2; Synthesis of 6-(2-oxopropyl)-4-(1H-pyrrol-2-yl)-2-thioxo-1,2-dihydropyrimidine-5-carbohydrazide (6)

A solution of pyrimidinethione **2** (2 mmol) and hydrazine hydrate (2.1 mmol, 80 %) in absolute ethanol (20 ml) was heated under reflux for 6 h. The excess solvent was evaporated under vacuum. The residue was recrystallized from ethanol. The obtained solid was collected and recrystallized from ethanol to afford compound **6** as brown crystals, mp. 236-238ºC, yield 51%. IR: 3410, 3312, 3166 (NH), 1715, 1662 (C=O), 1217 (C=S). ^{1}H-NMR: 10.35 (s, 1H, NH, CSNH, pyrim, exchangeable), 10.30 (s, 1H, NH, CONH, hydrazide, exchangeable), 8.40 (s, 1H, NH pyrrole exchangeable), 8.36-7.56 (m, 3H, pyrr-H), 4.73-6.62 (m, 2H, NH_2 exchangeable), 3.38 (s, 2H, CH_2CO), 2.17 (s, 3H, CH_3), EIMS (*m/z*, %): 291 ($M^{\cdot+}$, 30), 247 (41), 165 (32), 77 (100). Anal. Calc. for $C_{12}H_{13}N_5O_2S$ (291.19): C, 49.47; H, 4.50; N, 24.04. Found: C, 49.24; H, 4.21; N, 23.62.

Synthesis of 6-amino-7-methyl-4-(1H-pyrrol-2-yl)-2-thioxo-2,6-dihydropyrido[4,3-d]pyrimidin-5(1H)-one (7)

A mixture of pyrimidinethione **2** (2 mmol) and hydrazine hydrate (2.5 mmol, 80 %) was heated at 100ºC in neat for 2 h. The residue was triturated with ethanol to afford **7** as yellow crystals, mp. 210-212ºC, yield 51%. IR: 3410, 3312 (NH), 1673 (C=O), 1625 (C=N), 1217 (C=S). ^{1}H-NMR: 13.04 (s, 1H, NH, pyrim, exchangeable), 10.14 (s, 1H, NH, pyrr, exchangeable), 7.07-6.31 (m, 3H, pyrr-H), 5.52 (s, 2H, NH_2 pyrim), 5.10 (s, 1H, C_5-H pyrim), 2.19 (s, 3H, CH_3). EIMS (*m/z*, %): 257 (($M^{\cdot+}$-16) 30), 247 (20), 165 (32), 77 (100). Anal. Calcd. for $C_{12}H_{11}N_5OS$ (273.19): C, 52.73; H, 4.06; N, 25.62. Found: C, 52.64; H, 4.00; N, 25.46.

Synthesis of N'-benzylidene-6-(2-oxopropyl)-4-(1H-pyrrol-2-yl)-2-thioxo-1,2-dihydro-pyrimidine-5-carbohydrazide (8)

A mixture of hydrazide of pyrimidinethione **6** (2 mmol) and benzaldehyde (2.5 mmol, 80 %) was refluxed in boiling ethanol for 2 h. The residue was triturated with ethanol to afford **8** as yellow crystals, mp. 186-188-212ºC, yield 64%. IR: 3410, 3312 (NH), 1673 (C=O), 1625 (C=N), 1217 (C=S). ^{1}H-NMR: 13.04 (s, 1H, NH, pyrim, exchangeable), 10.14 (s, 1H, NH, pyrr, exchangeable), 7.07-6.31 (m, 3H, pyrr-H), 5.52 (s, 2H, NH_2 pyrim), 5.10 (s, 1H, C_5-H pyrim), 2.19 (s, 3H, CH_3). EIMS (*m/z*, %): 379 ($M^{\cdot+}$) 30), 347 (20), 270 (32), 215 (100), 156. Anal. Calcd. for $C_{19}H_{17}N_5O_2S$ (379.19): C, 60.14; H, 4.52; N, 18.46; S, 8.45. Found: C, 59.64; H, 4.30; N, 18.26; S, 8.26.

Synthesis of 6-(3-oxo-1-phenylbut-1-en-2-yl)-4-(1H-pyrrol-2-yl)-2-thioxo-1,2-dihydro-pyrimidine-5-carbohydrazide (9)

A solution of hydrazide of pyrimidinethione **6** (2 mmol) and benzaldehyde (2.1 mmol) in the presence of sodium ethoxide (0.005 mol) in ethanol (20 ml) was stirred in room tempreture for 6 h. The excess solvent was evaporated under vacuum. The residue was recrystallized from ethanol. The obtained solid was collected and recrystallized from ethanol to afford compound **9** as brown crystals, mp. 262-264ºC, yield 72%. IR: 3410, 3312, 3166 (NH), 1715, 1662 (C=O), 1217 (C=S). ^{1}H-NMR: 10.35 (s, 1H, NH, CSNH, pyrim, exchangeable), 10.30 (s, 1H, NH, CONH, hydrazide, exchangeable), 8.40 (s, 1H, NH pyrrole exchangeable), 8.36-7.56 (m, 3H, pyrr-H), 4.73-6.62 (m, 2H, NH_2 exchangeable), 3.38 (s, 2H, CH_2CO), 2.17 (s, 3H, CH_3), EIMS (*m/z*, %): 291 ($M^{\cdot+}$, 30), 247 (41), 165 (32), 77 (100). Anal. Calc. for $C_{19}H_{17}N_5O_2S$ (379): C, 60.14; H, 4.52; N, 18.46; S, 8.45. Found: C, 60.00; H, 4.36; N, 18.31; S, 8.29.

Synthesis of 2-benzoyl-6-(benzylideneamino)-7-methyl-4-(1H-pyrrol-2-yl)pyrido[4,3-d]pyrimidin-5(6H)-one (10)

A mixture of pyrimidinethione **7** (2 mmol), benzaldehyde (2 mmol) and (1mmol) sodium ethoxide was heated in boiling ethanol for 2 h. The residue was triturated with ethanol to afford **10** as yellow crystals, mp. 222-224ºC, yield 67%. IR: 3410, 3312 (NH), 1673 (C=O), 1625 (C=N), 1217 (C=S). ^{1}H-NMR: 13.04 (s, 1H, NH, pyrim, exchangeable), 10.14 (s, 1H, NH, pyrr, exchangeable), 7.07-6.31 (m, 3H, pyrr-H), 5.52 (s, 2H, NH_2 pyrim), 5.10 (s, 1H, C_5-H pyrim), 2.19 (s, 3H, CH_3). EIMS (*m/z*, %): 433 ($M^{\cdot+}$) 30), 247 (20), 165 (32), 77 (100). Anal. Calcd. for $C_{26}H_{19}N_5O_2$

(433): C, 72.04; H, 4.42; N, 16.16. Found: C, 71.84; H, 4.23; N, 16.00.

Synthesis of (6-amino-7-methyl-5-oxo-4-(1H-pyrrol-2-yl)-5,6-dihydropyrido[4,3-d]pyrimidin-2-yl) 2-chloroethanethioate (11)

A mixture of pyrimidinethione **10** (2 mmol) and choloroacetylchloride (2 mmol) was heated in dry pyridine for 2 h. The residue was triturated and pour into HCl/ice and crystalized from ethanol to afford **11** as yellow crystals, mp. 182-184ºC, yield 63%. IR: 3410, 3312 (NH), 1673 (C=O), 1625 (C=N), 1217 (C=S). ^{1}H-NMR: 13.04 (s, 1H, NH, pyrim, exchangeable), 10.14 (s, 1H, NH, pyrr, exchangeable), 7.07-6.31 (m, 3H, pyrr-H), 5.52 (s, 2H, NH_2 pyrim), 5.10 (s, 1H, C_5-H pyrim), 2.19 (s, 3H, CH_3). EIMS (*m/z*, %): 349 ($M^{\cdot+}$) 30), 247 (20), 165 (32), 77 (100). Anal. Calcd. for $C_{14}H_{12}ClN_5O_2S$ (349): C, 48.07; H, 3.46; Cl, 10.13; N, 20.02; S, 9.17. Found: C, 47.84; H, 3.23; Cl, 9.92; N, 19.80; S, 8.92 .

Biological evaluation:

Cell Culture:

liver Cancer cell line of human origin HepG-2 (human hepatocellular carcinoma) Cells were routinally cultured in DMEM media (Lonza), supplemented with 10%FBS (Lonza), 1%100u/ml penicillinand 100ug/ml streptomycin(Lonza) in a humidified incubator at 37ºC with an atmosphere containing 5%CO_2. Every experiment was carried out in triplicate. At 85% confluence cells were harvested using 0.25% trypsin and were subculture into 75 cm^2 and six –well plates or 96 –well plates according to selection of experiments. Cells were allowed to attach to the surface for 24 hours prior to treatment. Pyrimidin-2-thione derivatives were dissolved in DMSO and diluted to appropriate concentrations.

Cytotoxicity evaluation against HepG-2 cell line:

The viability of control and treated cells were evaluated using the MTT assay in triplicate. MTT assay is a laboratory test and a standard colorimetric assay (an assay which measures changes in color) for measuring cellular growth, Yellow MTT (3-(4,5-Dimethylthiazol-2-yl) -2, 5-diphenyltetrazolium bromide, a tetrazole) was reduced to purple formazan in the mitochondria of living cells. A solubilization solution (dimethyl sulfoxide) was added to dissolving the insoluble purple formazan product into a colored solution. Briefly, HepG2 (hepatocellular carcinoma cell line) was seeded in 96-well plates containing 100µl of the growth medium at a density of (1x104) cells/well. Cells were permitted to adhere for 24h till confluence, washed with PBS, and then treated with different concentration of compounds in fresh maintenance medium from 500 to 15.63 µg and incubated at 37ºC for 24h. A control of untreated cells was made in the absence of the test compound. Untreated cells used as negative control. Serial two-fold dilutions of the tested compounds were added into a 96-well tissue culture plate using a multichannel pipette (Eppendorff, Germany). After treatment (24h), the culture supernatant was replaced by fresh medium. Then, the cells in each well were incubated at 37˚C with 100µl of MTT solution (5mg/ml) for 4h. After the end of incubation, the MTT solution was removed, and then 100µl of DMSO was added to each well. The absorbance was detected at 570 nm using a microplate reader (SunRise TECAN, Inc, USA) [xxi].

Gamma Irradiation with the derivative:

Gamma irradiation was performed at the National Centre for Radiation Research and Technology (NCRRT), Egyptian Atomic Energy Authority (EAEA), Cairo, Egypt, using Canadian Gamma Cell-40 biological irradiator (137 Cesium), manufactured by the Atomic Energy of Canada Limited, Ontario, Canada. The radiation dose rate was 0.61 Gy/ min at the time of exposure. HepG2 cells were irradiated with 8 Gy with or without the selected derivative. The dose calculated according to the Dosimeter department in the NCRRT.

Quantification of p21 and caspase-3 gene expression & Oxidative stress evaluation:

The parameters were estimated in the following groups:

1. Control (HepG-2 cells without treatment).
2. IC50 x2 (HepG-2 cells treated with IC50 x 2 = 51 µg/ml, then the cells were harvested after two times intervals 24 hr and 48 hr).
3. IC50 (HepG-2 cells treated with IC50 = 25.5 µg/ml, then the cells were harvested after two times intervals 24 hr and 48 hr).
4. ½ IC50 (HepG-2 cells treated with IC50 = 12.75 µg/ml, then the cells were harvested after two times intervals 24 hr and 48 hr).
5. RAD (HepG-2 cells irradiated with 8 Gy, then the cells were harvested after two time intervals 24 hr and 48 hr).
6. RAD + IC50 x2 (HepG-2 cells irradiated with 8 Gy + treated with IC50 = 51 µg/ml, then the cells were harvested after two times intervals 24 hr and 48 hr).
7. RAD + IC50 (HepG-2 cells irradiated with 8 Gy + treated with IC50 = 25.5 µg/ml, then the cells were harvested after two times intervals 24 hr and 48 hr).
8. RAD + ½ IC50 (HepG-2 cells irradiated with 8 Gy + treated with IC50 = 12.75 µg/ml, then the cells were harvested after two times intervals 24 hr and 48 hr).

Real-time polymerase chain reaction (RT-PCR):

To analyze gene expression of the cell cycle inhibitor p21 and caspase-3. Total RNA was extracted from the collected cell suspension using RNeasy Mini Kit (Qiagen, Cat. No. 74104) according to the manufacturer's instructions. First strand complementary DNA (cDNA) synthesis was performed using QuantiTect Reverse Transcription Kit (Qiagen, Cat. No. 205311) according to the manufacturer's instructions using 1µg RNA as a template. RT-PCR were performed in a thermal cycler step one plus (Applied Biosystems, USA) using the Sequence Detection Software (PE Biosystems, CA). The primers utilized in these experiments are listed in **Table 3**. The reaction mixture of total volume 25 µl was consisting of 2X SYBR Green PCR Master Mix (Qiagen, Cat. No. 204143), 900 nM of each primer and 2µL of cDNA. PCR thermal-cycling conditions included an initial step at 95°C for 5 min; 40 cycles at 95°C for 20s, 60°C for 30s, and 72°C for 20s. The relative expression of the real-time reverse transcriptase PCR products was determined by the ΔΔCt method. This method calculates a relative expression to housekeeping gene using the equation: fold induction = 2-(ΔΔCt). Where ΔΔ Ct=Ct [gene of interest (unknown sample)-Cthousekeeping gene (unknown sample)] - [Ct gene of interest (calibrator sample)-Ct housekeeping gene (calibrator sample)] [xxii].

Determination of plasma Malondialdehyde (MDA):

Lipid peroxidation in cells was measured by spectrophotometric analysis of MDA based on its reaction with thiobarbituric acid using Colorimetric kit supplied by biodiaganostic, 29 El-Tahrer St. - Dokki- Giza – Egypt.

Determination of Reduced Glutathione (GSH):

GSH was assayed based upon the development of a relatively stable yellow color when 5,5'-dithiobis-(2-nitrobenzoic acid) is added to sulphdril compounds using Colorimetric kit supplied by biodiaganostic, 29 El-Tahrer St. - Dokki- Giza – Egypt.

Table 1: primer sequences for the genes amplified.

Gene	Strand	Sequence 5` - 3`	Product length (bp)	Ref. Seq.
cyclin-dependent kinase inhibitor p21	F	GCACAAGGGTACAAGACAGTG	220	NM_001291549
	R	CGATGGAACTTCGACTTTGTCA		
caspase 3 (CASP3)	F	AGA ACT GGA CTG TGG CAT TGA G	191	NM_004346
	R	GCT TGT CGG CAT ACT GTT TCA G		
GAPDH	F	AGGGGCCATCCACAGTCTTC	258	NM_001357943
	R	AGAAGGCTGGGGCTCATTTG		

2. Results and discussion :

2.1. Chemistry

Herein, Pyrimidinthione **2** was efficiently prepared *via* ultrasonic irradiation cyclocondensation reaction of pyrazole aldehyde, ethyl 3,5-dioxohexanoate and thiourea and utilized as a key building block synthon for construction of valuable *N*-heterocycles. The structure of pyrimidinthione **2** was established on its analytical and spectral data. Pyrimidine **2** could be existed because of this thermodynamic structure than pyridinthione **1** (Scheme 1) [3-6].

The reaction of **2** with ethyl chloroacetate under different conditions was studied and found to afford thiazolopyrimidine derivative **4** as a sole product (Scheme 2). The formation of **4** could be explained *via* formation of the *S*-alkylated product **3** in first pursued by 1,5-exo-trig cyclization to eliminate ethanol molecule.

It was fortunate that, reaction of pyrimidine **2** with chloroacetyl chloride was mainly dependent on the reaction conditions. Indeed, in refluxing potassium hydroxide/ethanol, thiazolopyrimidine derivative **4** was obtained as sole product. The structures of all products were substantiated from their analytical and spectral data. The IR spectrum of compound **4** showed ν C=O of thiazolidinone ring at 1707 cm^{-1}. In turn, hydrazinolysis of pyrimidine **2** failed to give the expected hydrazinopyrimidine **5** and led to the formation of pyrimidinthion-hydrazide **6** and N-aminopyridonopyrimidinthione **7** when the reaction was carried out in refluxing ethanol and in neat, respectively. The structure of compounds **6** and **7** was supported by elemental and spectral analysis. The formation of compounds **6** and **7** could be visualized to occur *via* Scheme 3. Reaction of the hydrazide **6** with benzaldehyde in different reaction condition afforded hydrazone **8** and chalcone **9**. Increasing the polarity of medium (e.g. using ethoxide versus ethanol) enhanced the C-C bond formation that is more thermodynamic control than C-N- bond formation and promoted to afford high percentage yield of Chalcone **9** versus formation of kinetic product hydrazone **8.** On the other hand, reaction of the pyrimidin-2-thione **7** with different carbon electrophiles e.g. benzaldehyde and chloroacetylchloride afforded 2-benzoylpyrimidine with desulfurization **10** and S-acylation product **11** respectively (Scheme 4). The

formation of product **13** can be explained via Scheme 5

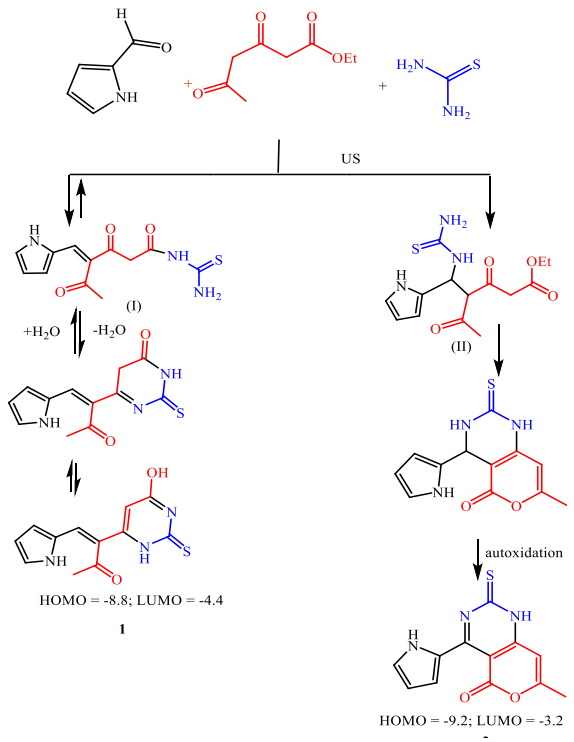

Scheme 1. Synthesis of pyrimidin-thione **2**.

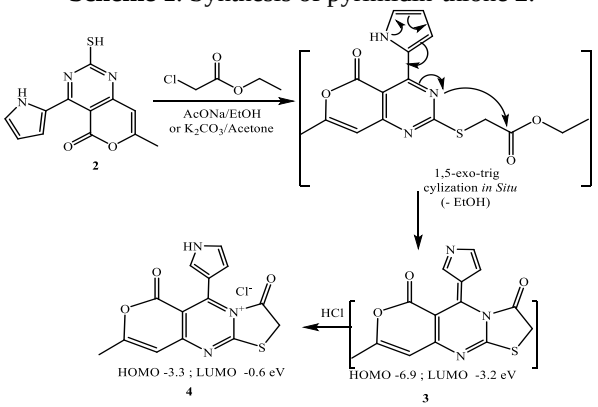

Scheme 2. Reaction of pyrimidinethione **2** with ethyl chloroacetate.

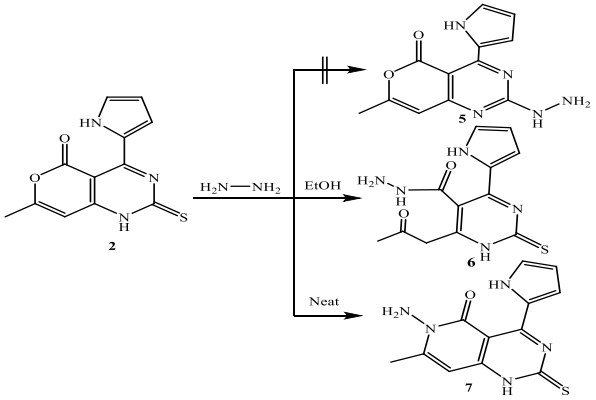

Scheme 3. Hydrazinolysis of pyrimidine **2**.

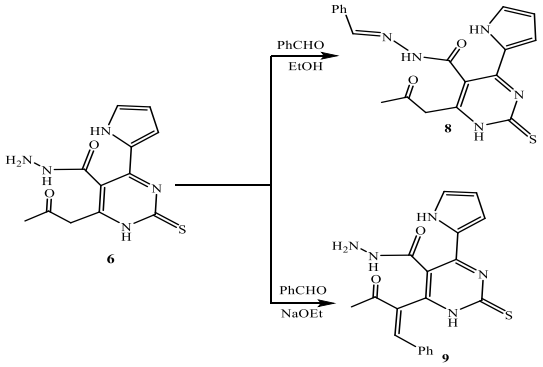

Scheme 4; Reaction of hydrazide **9** with benzaldehyde in neutral and basic conditions

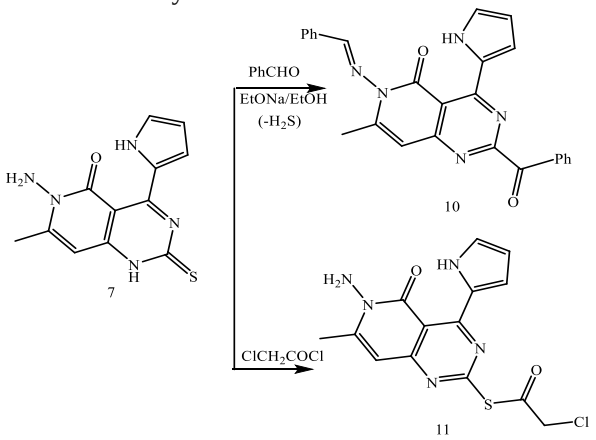

Scheme 5; Reaction of the pyrimidin-2-thione **10** with benzaldehyde and chloroacetylchloride

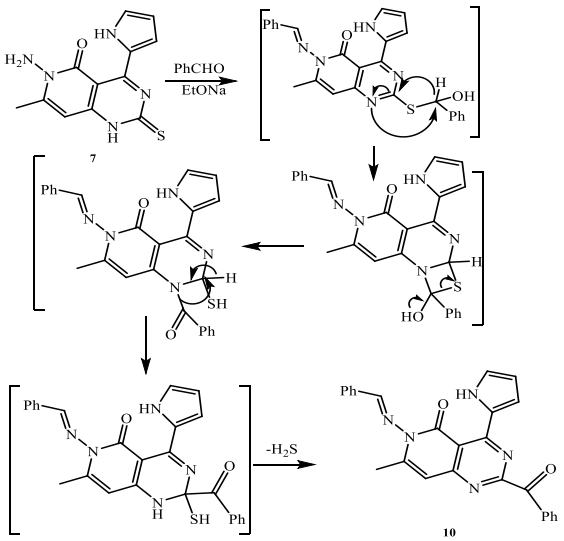

Scheme 6; Outline mechanism of formation the 2-benzoylpyrimidine derivative **10**

2.2. Computational studies (DFT methods)

DFT studies were carried out for the synthesized compounds using Materials Studio 6.0 (MS 6.0) software from Accelrys, Inc. DMol3 module was used to perform the DFT calculations using Perdew and Wang LDA exchange-correlation functional and DND basis set [28-33]. The calculated parameters involved the electron density, dipole moment and Frontier molecular orbitals and the molecular surface area [34,35]. Frontier molecular orbitals include the highest occupied molecular orbitals (HOMOs) and the lowest unoccupied molecular orbitals (LUMOs) [36,37]. The molecular structures of the synthesized compounds are superior to be formed to a stable geometry is known as optimization. Such the energy of the structure is transported to a stationary point, the geometry of the compounds as an example, compounds of pyrimidine-thione is gradually optimized, and its energy is continuously decreased until the fluctuations in the molecule energy are minimized. Frontier molecular orbitals possess the highest occupied molecular orbital (HOMO) and the lowest unoccupied molecular orbital (LUMO) (**Figures 1** and **2**). The regions of highest electron density (HOMO) characterizes the electrophilic-attacking sites, while the LUMO imitates the nucleophilic-attacked sites [38-40]. The quantum chemical computation could be explained this reaction at the different conditions afforded different products **2-11**. The regioselective multicomponent reaction preferred to attack the ethyl 4-((1H-pyrrol-2-yl)(thioureido)methyl)-3,5-dioxohexanoate intermediate (I) that has lower Δ E= LUMO- $HOMO_1$ = 2.930 eV than 4-((1H-pyrrol-2-yl)methylene)-N-carbamothioyl-3,5-dioxohexanamide intermediate (II) that has Δ E= LUMO- $HOMO_1$ = 5.664 eV using electron rich aryl groups to afford the desired product pyrimidine-2-thione (2) (see more in Scheme 1 and **Table 2**). Also, **Fig. 1** indicated the thermodynamic stability of the pyrimidine thione products that are preferred to yield in the thermal and ultrasonic reaction conditions. On the other hand, the dipole moment (μ) is a promising measurable parameter for the molecular polarity, it is clearly evident from **Table 3** that compounds **4**, **8** and **10** exhibit high polarities and the possibility of binding with anticancer arginine 265 which in turn favored. So, they are most potent anticancer activity. The hydration energy can be echoed the more solvated parts of synthesized compounds that be contributed to attack the insect resulting in most potent activity for such compounds (**Table 4**). For more confirmation, the nucleophilicity index (ω) as well as the surface area, follow the order: **10** >**4**> **8**> **9** are in conformity to anticancer activity. Accordingly, the DFT data run in harmony with the previous obtained results.

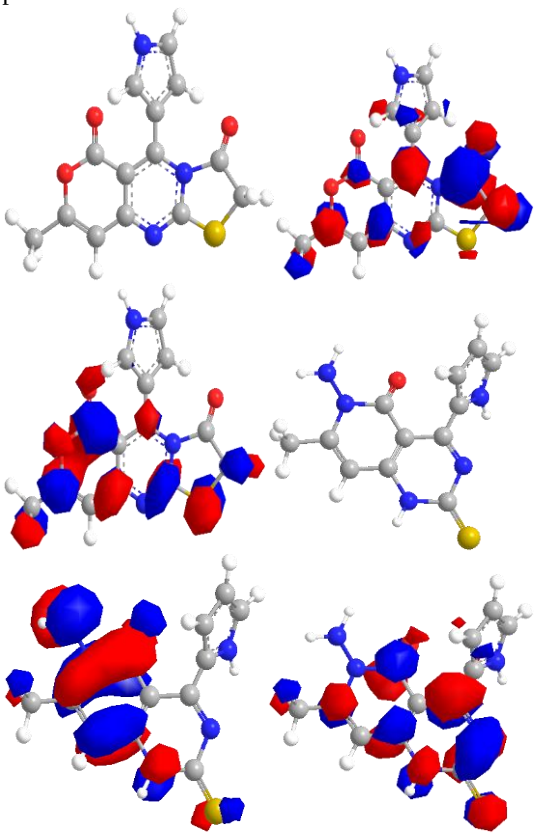

Figure 1: Optimized structure of the compounds **4** and **10** (left), HOMO (middle) and LUMO (right) for most potent anticancer compounds. Color index: White H, Grey C, Blue N, Red O and yellow S.

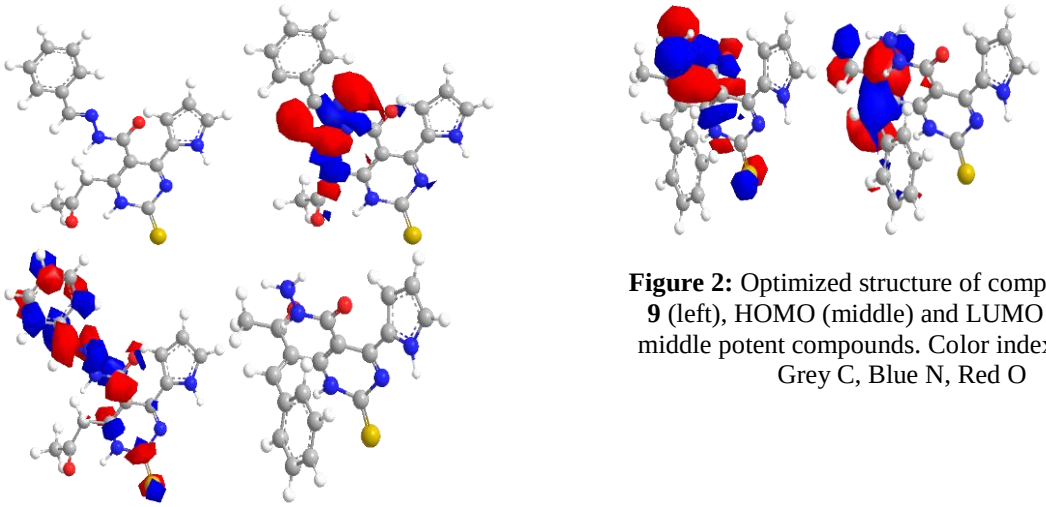

Figure 2: Optimized structure of compounds **8** and **9** (left), HOMO (middle) and LUMO (right) for middle potent compounds. Color index: White H, Grey C, Blue N, Red O

Table 2: DFT parameters calculated for the synthesized compounds.

Comp. No	E HOMO (eV)	ELUMO (eV)	ΔE (LUMO-HOMO)	Dipole moment μ (Debye)	Hydration E (k cal mol^{-1}	Surface area, A,(nm^2)	Electrophilicity, ω (eV)
2	-5.795	-0.181	5.634	-0.526	-20.691	1183.34	2.12
4	-2.850	-0.810	2.040	13.879	-55.453	1354.25	5.24
8	-2.829	-0.220	2.609	4.733	-59.942	1187.32	3.27
9	-4.632	-1.451	3.280	12.318	-53.321	1209.58	2.61
10	-2.971	-1.533	1.442	12.256	-53.272	1126.34	5.47

2.3. Anticancer evaluation

The results showed that the new Pyrimidin-2-thione derivative was able to cause cell cycle arrest at least partly through down-regulation the expression level of the cell cycle inhibitor p21 and induced cancer cell apoptosis via caspase-3 dependent pathway. The results indicated that the irradiation plus the derivative is more effective than the derivative only. The irradiation reinforced the effect of the derivative. As the lower dose from the derivative plus irradiation is more effective than the higher dose of derivative only.

p21 can be considered a negative regulator of the p53-dependent apoptosis and it was suggested to be able to induce growth arrest if DNA damages are slight. When damages are more serious, p53 can directly induce apoptosis. In fact, prolonged treatments of cancer cells with DNA damaging agents, determine a p21 inactivation mediated by caspase-3 cleavage and reduction of p21 levels resulted in apoptosis [xxiii]. Caspase-3 is the most frequently activated cysteine protease, which plays a vital role in both intrinsic and extrinsic apoptotic pathways. Thus, caspase-3 has been recognized as a reliable molecular biomarker for cell apoptosis [xxiv].

While the results of the Oxidative stress markers (GSH and MDA) showed that GSH increase in the cells treated with the Pyrimidin-2-Thione derivative only but decrease with irradiation. However, the cells irradiated and treated with the Pyrimidin-2-Thione derivative showed higher GSH in compare with cells exposed to the ionizing radiation only. GSH is critical to fight against oxidative stress [xxv]. On the other hand, MDA decrease in the cells treated with the Pyrimidin-2-Thione derivative only, but increase with irradiation. However, the cells irradiated and treated with the Pyrimidin-2-Thione derivative showed lower MDA in compare with cells exposed to the ionizing radiation only. MDA indirectly evaluating the degree of cell damage [xxvi, xxvii].

Table 3: *In vitro* anticancer activity of Pyrimidin-2-Thione derivatives 2,4,10 and doxorubicin as stander drug against HepG-2 (human hepatocellular carcinoma) Cells.

Compounds	IC50(μg/ml)
4	93.9± 3.2
8	190 ± 5.9
10	25.5 ± 1.3
Doxorubicin	0.36±0.02

As Compound **10** was the most active against the liver carcinoma cell line (HepG-2) its cytotoxicity was evaluated against normal rat hepatocytes. it showed weak cytotoxic effects using MTT assay under the same experimental conditions for 48 hrs incubation with CC50 = 1877.5 μg/ml (= > 500 μg/ml) .

Table 4: p21 gene expression, caspase-3 gene expression, GSH content and MDA in different groups after 24 hr and 48 hr.

Parameters / Groups	P21 (fold)		Caspase 3 (fold)		GSH (mmol / g. tissue)		MDA (nmol / g.tissue)	
	24 hr	**48 hr**	**24 hr**	**48 hr**	**24 hr**	**48 hr**	**24 hr**	**48 hr**
Control	1.0±0.03	**1.0±0.01**	1.0±0.02	**1.02±0.03**	68±18	**69.4±9.1**	122±7.6	**114.1±3.1**
IC50 x2	0.63±0.02*	**0.31±0.09*****	5.0±2.5*	**7.8±0.68*****	108±6.2***	**129±7.2*****	62±26*	**42.6±8.8*****
IC50	0.61±0.1**	**0.44±0.07*****	4.9±0.62	**6.4±0.31****	88±4.3	**109.1±4.5*****	79±22	**60.2±11.1*****
½ IC50	0.60±0.12**	**0.55±0.04*****	3.3±0.70	**4.9±0.25***	81±5.7	**99.4±9.8****	91±11	**88.3±8.1**
RAD	0.37±0.13***	**0.2±0.03*****	7.8±1.4***	**8.5±1.24*****	21±2.4***	**38.7±3.9****	212±32***	**205.3±9.8*****
RAD + IC50 x2	0.33±0.11***	**0.14±0.02*****	10±1.2***	**13±0.81*****	69±12	**108±9.7*****	159±22	**136.7±18.1**
RAD + IC50	0.49±0.20***	**0.34±0.05*****	8.9±0.35***	**11.3±2.2*****	56±3.6	**83.6±9**	174±15	**156.1±13.1****
RAD + ½IC50	0.52±0.08**	**0.26±0.04*****	6.7±2.2**	**8.6±2.14*****	51±7.3	**80.3±11.2**	196±2.3**	**168.1±11.2*****

Each value represents the mean ± standard deviation.* Significant difference versus control group at p≤0.05.

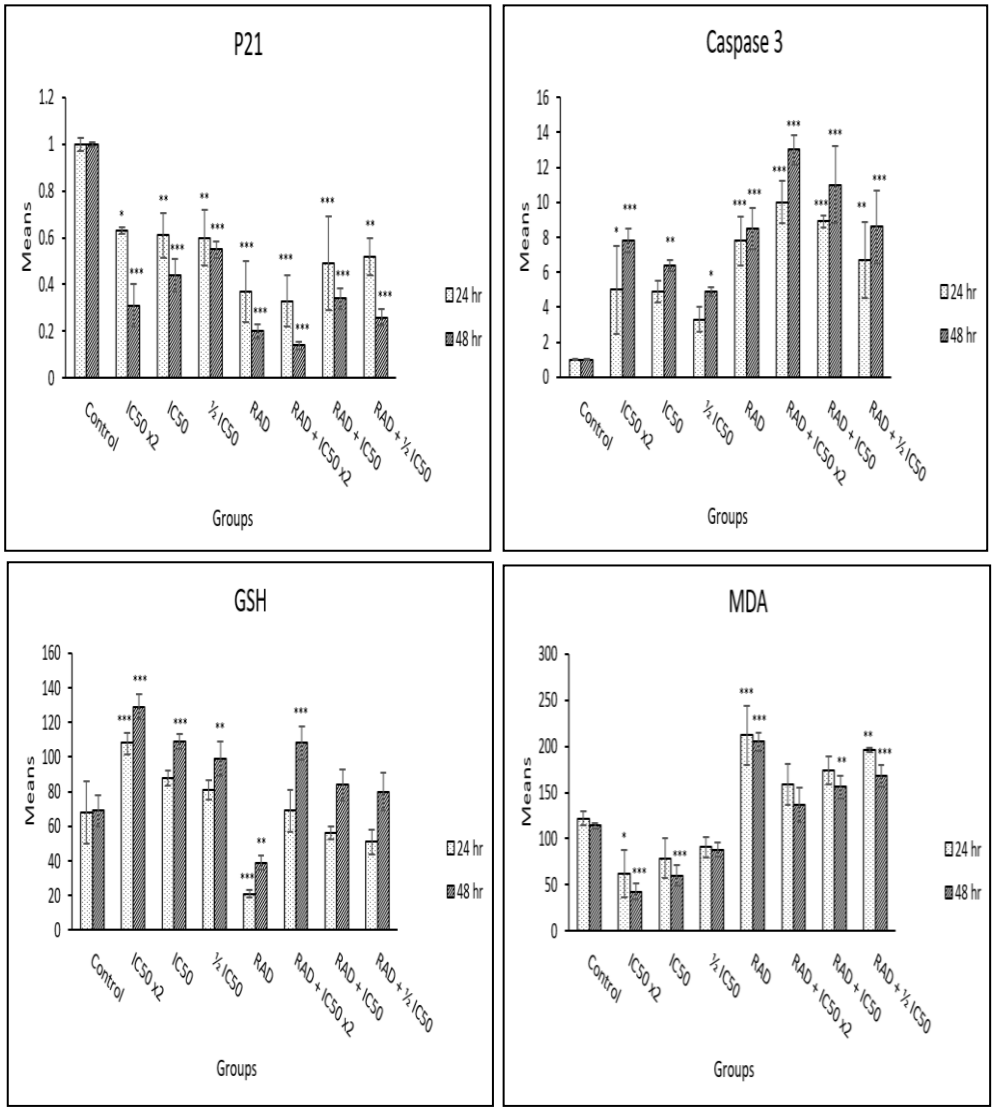

Figure 3. p21 gene expression, caspase-3 gene expression, GSH content and MDA in different groups after 24 hr and 48 hr.

CONCULSION

Synthesis and anticancer evaluation of some new Pyrimidin-2-Thione derivatives **2-11**. The most potent derivative **10** showed much better activity was produced via simple, two-step, and ecofriendly synthetic protocols. Qualified study was concerning the result density function theory (DFT) has thru on grinding and ultrasound-assisted

tools. All Pyrimidin-2-Thione structures can be elucidated by elemental and spectral data. The new derivative of the Pyrimidin-2-Thione compound has an effective anti-cancer effect and it was found that using the new compound with ionizing radiation at a dose of 8 Gy improves the effectiveness of the compound on liver cancer cells. The new Pyrimidin-2-Thione derivative was able to cause cell cycle arrest at least partly by down regulating the expression level of the cell cycle inhibitor p21 and up regulating caspase 3 Inducing cancer cell apoptosis via caspase-3 dependent pathway.

References

[i] Sujith, K. V., Rao, J. N., Shetty, P., & Kalluraya, B. (2009). Regioselective reaction: synthesis and pharmacological study of Mannich bases containing ibuprofen moiety. *European journal of medicinal chemistry*, *44*(9), 3697-3702.

[ii] Isloor, A. M., Kalluraya, B., & Shetty, P. (2009). Regioselective reaction: synthesis, characterization and pharmacological studies of some new Mannich bases derived from 1, 2, 4-triazoles. *Euro. j. med. chem.*, *44*(9), 3784-3787.

[iii] Rizk, S. A., Abdelwahab, S. S., & Sallam, H. A. (2018). Regioselective Reactions, Spectroscopic Characterization, and Cytotoxic Evaluation of Spiro-pyrrolidine Thiophene. *J. Het. Chem. 55*(7), 1604.

[iv] Rizk, S.A.; Shaban, S.A (2019). Facile One-pot Synthesis and Anticancer Evaluation of Interesting Pyrazole and Pyrimidinthione via Heterocyclic Interconversion. J. Het. Chem., 56, 2379.

[v] Rizk, S. A.; Abdelwahab, S. S.; Elrazaz, E. (2019). Synthesis and QSAR Study of Some Novel Heterocyclic Derivatives as In Vitro Cytotoxic Agents. J Het. Chem, 56, 443.

[vi] Fahmy, A.F.M., Rizk, S.A., Hemdan, M.M., El-Sayed, A.A., Hassaballah, A.I. (2018) Efficient Green Synthesis and Computational Chemical Study of Some Interesting Heterocyclic Derivatives as Insecticidal Agents. J. Het. Chem., 55, 2545-2555.

[vii] Larhed, M., & Hallberg, A. (2001). Microwave-assisted high-speed chemistry: a new technique in drug discovery. *Drug discovery today*, *6*(8), 406-416.

[viii] Lidström, P., Tierney, J., Watheyb, B., & Westmana, J. (2001). Microwave assisted organic synthesisÐa review. *Tetrahedron*, *57*, 9225-9283.

[ix] Sasikumar, A., Mohanasrinivasan, V., Ajeesh Kumar, A. K., & Krishnaswamy, D. (2018). Design, synthesis, and evaluation of the anticancer properties of a novel series of α-(benzoylamino)-β-substituted acrylic amide derivatives of pyrazolo [1, 5-a] pyrimidine. Journal of Heterocyclic Chemistry, 55(1), 214-225.

[x] Amin K.M, Eissa A.M, Abou-Seri S.M, Awadallah F.M, Hassan G.S. (2013). Synthesis and biological evaluation of novel coumarinpyrazoline hybrids endowed with phenylsulfonyl moiety as antitumor agents.Eur. J. Med. Chem.,60:187-198.

[xi] Nasr T, Bondock S, Youns M. (2014). Anticancer activity of new coumarin substituted hydrazide-hydrazone derivatives. Eur. J. Med. Chem.,76:539-548.

[xii] Kim, R., Tanabe, K., Uchida, Y., Emi, M., Inoue, H., & Toge, T. (2002). Current status of the molecular mechanisms of anticancer drug-induced apoptosis. Cancer chemotherapy and pharmacology, 50(5), 343-352.

[xiii] Vermes, I., Haanen, C., & Reutelingsperger, C. (2000). Flow cytometry of apoptotic cell death. Journal of immunological methods, 243(1), 167-190.

[xiv] Thornberry, N. A. (1998). Caspases: key mediators of apoptosis. Chemistry & biology, 5(5), R97-R103.

[xv] Gartel, A. L., & Radhakrishnan, S. K. (2005). Lost in transcription: p21 repression, mechanisms, and consequences. Cancer research, 65(10), 3980-3985.

[xvi] Hanahan, D. & Weinberg R. A. (2000). The hallmarks of cancer. Cell 100: 57–70.

[xvii] Scharf, G., Prustomersky, S., Knasmüller, S., Schulte-Hermann, R., & Huber, W. W. (2003). Enhancement of glutathione and γ-glutamylcysteine synthetase, the rate limiting enzyme of glutathione synthesis, by chemoprotective plant-derived food and beverage components in the human hepatoma cell line HepG2. *Nutrition and cancer*, *45*(1), 74-83.

[xviii] Martin, M. A., Ramos, S., Mateos, R., Granado Serrano, A. B., Izquierdo-Pulido, M., Bravo, L., & Goya, L. (2008). Protection of human HepG2 cells against oxidative stress by cocoa phenolic extract. *Journal of agricultural and food chemistry*, *56*(17), 7765-7772.

[xix] Song D., (2020). Effects of nalmefene combined with hyperbaric oxygen therapy on serum levels of S100β protein,hypoxi-inducible factor-1α,malondialdehyde and lactate in acute severe craniocerebral injury[J]. Anhui Medical and Pharmaceutical Journal ,28(1):47-50.

[xx] Ji Z S,Wu Q,Liu X Y., (2019). The application of epalrestat in the protection of MDA,SOD,TAC and

endothelial function in early diabetic retinopathy[J]. Chinese Journal of Health Care and Medicine, 21(6):514-517.

[xxi] Wilson, A. P. (2000). Cytotoxicity and viability assays. *Animal cell culture: a practical approach*, *3*, 175-219.

[xxii] Livak, K. J., Schmittgen, T. D. (2001). Analysis of relative gene expression data using real-time quantitative PCR and the 2− ΔΔCT method. methods. 25(4), 402-408.

[xxiii] Zhang, Y., Fujita, N., & Tsuruo, T. (1999). Caspase-mediated cleavage of p21 Waf1/Cip1 converts cancer cells from growth arrest to undergoing apoptosis. Oncogene, 18(5), 1131-1138.

[xxiv] Khalilzadeh, B., Shadjou, N., Charoudeh, H. N., & Rashidi, M. R. (2017). Recent advances in electrochemical and electrochemiluminescence based determination of the activity of caspase-3. Microchimica Acta, 184(10), 3651-3662.

[xxv] Martin, M. A., Ramos, S., Mateos, R., Granado Serrano, A. B., Izquierdo-Pulido, M., Bravo, L., & Goya, L. (2008). Protection of human HepG2 cells against oxidative stress by cocoa phenolic extract. *Journal of agricultural and food chemistry*, *56*(17), 7765-7772.

[xxvi] Song D., (2020). Effects of nalmefene combined with hyperbaric oxygen therapy on serum levels of S100β protein,hypoxi-inducible factor-1α,malondialdehyde and lactate in acute severe craniocerebral injury[J]. Anhui Medical and Pharmaceutical Journal ,28(1):47-50.

[xxvii] Ji Z S,Wu Q,Liu X Y., (2019). The application of epalrestat in the protection of MDA,SOD,TAC and endothelial function in early diabetic retinopathy[J]. Chinese Journal of Health Care and Medicine, 21(6):514-517.

[28] El-Hashash, M. A.; Rizk, S. A. (2016) Regioselective Diastereomeric Michael Adducts as Building Blocks in Heterocyclic Synthesis. J. Het. Chem, 53,1236-1240.

[29]El-Hashash, M.; Rizk, S.; Aburzeza, M. Utility of p-Acetamidobenzoyl Prop-2-enoic Acid in the Synthesis of New α-Amino Acids and Using Them as Building Blocks in Heterocyclic Synthesis (2011) Egypt J Chem,54, 299.

[30] Rizk, S.; El-Hashash, M.; Mostafa, K. (2008) Utility of β-aroyl acrylic acid in heterocyclic synthesis Egypt J. Chem., 51(5), 611.

[31] Rizk, S. A.;El-Hashash, M.; Elbadawy A.A. (2017) Ultrasonic and Grinding Aptitudes of One-Pot Synthesis of 5-(4-Chlorophenyl)-7-(3,4-Dimethyl Phenyl)-2-oxo-2H-Pyrano[2,3-b]Pyridine Derivatives as Antibacterial Agents J. Het. Chem., 54, 2003.

[32] El-Hashash, M.; Rizk, S. A.; El-Badawy A. (2018) Ultrasonic Aptitude of Regioselective Reaction of 6-bromo-spiro-3,1-benzoxazinone2,1′-isobenzofuran-3′,4-dione Towards Some Electrophilic and Nucleophilic Reagents. J. Het. Chem., 55, 2090-2098.

[33] Rizk S.A.; El-Sayed G.A.; El-Hashash, M. (2018) One-pot synthesis, spectroscopic characterization and DFT study of novel 8-azacoumarin derivatives as eco-friendly insecticidal agents. J. Iranian Chem. Soc. 15, 2093–2105.

[34] Attia, S.K..; El-Gendy, A.T.; Rizk, S.A. (2019) Efficient green synthesis of antioxidant azacoumarin dye bearing spiro-pyrrolidine for enhancing electro-optical properties of perovskite solar cells. J. Mol. Struct. 1184, 583.

[35] El-Hashash, M.A.; Rizk, S.A.; El-Naggar, A.M.; El-Bana, M.G. (2017) Regiospecific Isomerization of 2-Benzoxazinon-2-yl Benzoic Acid Toward Some Nitrogen Nucleophiles as Environmental Insecticide . J. Het. Chem. 54, 3716-3724.

[36] El-Hashash, M.A.; Darwish, K.M.; Rizk, S.A.; El-Bassiouny, F.A. (2011)The uses of 2-ethoxy-(4H)-3,1-benzoxazin-4-one in the synthesis of some quinazolinone derivatives of antimicrobial activity. Pharmaceuticals, 4(7), 1032-1051.

[37] Elgendy, A.T, Youssef, A, Rizk, S. A, (2020). Which Energetically Favorable Sustainable Synthesis of 4-amino-8-azacoumarin ester or 4-hydroxy-3-cyano derivative Based on New Exact Kinetic Arrhenius and DFT Stimulation. J. Iranian Chem. Soc. 17, 1001.

[38] El-Hashash, M.A.; Rizk, S.A.; El-Bassiouny, F.A.; Guirguis, D.B.; Khairy, S.M.; Guirguis, (2017). Facile Synthesis and Structural Characterization of Some Phthalazin-1(2H)-one Derivatives as Antimicrobial Nucleosides and Reactive Dye. Egypt J. Chem. 60, 407.

[39] Elkholy, A.E., Rizk, S.A., Rashad, A.M. (2019) Enhancing lubricating oil properties using novel quinazolinone derivatives: DFT study and molecular dynamics simulation. J. Mol. Struct., 1175, 788.

[40] Heakal, F. E.; Attia, S.K.; Rizk, S.A.; Abou Essa, M.A.; Elkholy, A.E. (2017) Synthesis, characterization and computational chemical study of novel pyrazole derivatives as anticorrosion and antiscalant agents. J. Mol. Struct. 1147, 714.